Computer-Aided Civil and Infrastructure Engineering **20** (2005) 408–423

A Wavelet-Based Approach to Identifying Structural Modal Parameters from Seismic Response and Free Vibration Data

C. S. Huang,* S. L. Hung, C. I. Lin & W. C. Su

Department of Civil Engineering, National Chiao Tung University,1001 Ta-Hsueh Road, Hsinchu, Taiwan 30050

Abstract: *This work presents the use of a discrete wavelet transform to determine the natural frequencies, damping ratios, and mode shapes of a structure from its free vibration or earthquake response data. The wavelet transform with orthonormal wavelets is applied to the measured acceleration responses of a structural system, and to reconstruct the discrete equations of motion in various wavelet subspaces. The accuracy of this procedure is numerically confirmed; the effects of mother wavelet functions and noise on the ability to accurately estimate the dynamic characteristics are also investigated. The feasibility of the present procedure to elucidate real structures is demonstrated through processing the measured responses of steel frames in shaking table tests and the free vibration responses of a five-span arch bridge with a total length of 440 m.*

1 INTRODUCTION

Identifying the dynamic characteristics of a structure from field measurements is crucial because the identified modal parameters can not only be used to validate or update the finite element model established in the design stage, but also to assess damage to a structure caused by severe loading, like a strong earthquake, or by deterioration of the material. Although spectral analysis in frequency domain provides an easy method for identifying modal parameters, the loss of accuracy engendered with FFT and noise on estimating the spectra of measured responses and input forces causes the incorrectness of the identified results, especially for highly damped systems and systems with severe modal interference. Conventional techniques in the time domain, such as the time series approach associated with the ARX or ARMAX model (Safak and Celebi, 1991; Loh and Lin, 1996; Satio and Yokota, 1996) and the subspace approach (VanDerVeen et al., 1993; Huang and Lin, 2001) have been often applied to determining the dynamic characteristics of a structure from its seismic responses. The Ibrahim time domain method (Ibrahim and Mikulcik, 1977), the complex exponential approach (Brown et al., 1979), and the polyreference method (Vold et al., 1982) have been frequently used to process free vibration data.

In recent years a new and powerful mathematical tool called wavelet transformation has been developed, the history of whose development can be found in introductory articles (Flandrin, 1990; Strang, 1993) and books (Combes et al., 1990; Barbara, 1996). Unlike a Fourier transform, which expresses a signal in terms of frequency components, the wavelet transform decomposes a signal into frequency components that are functions of time. The advantages of the wavelet transformation over the Fourier transformation have been addressed in several articles and books (Strang, 1993; Combes et al., 1990; Barbara, 1988). The wavelet transformation has been successfully applied in mathematics, physics, medicine, biology, and engineering, especially for signal processing and solving nonlinear problems. Such applications have been reviewed in various articles (Jawerth and Sweldens, 1994; Unser and Aldroubi, 1996; Kobayashi, 2001).

The wavelet transformation also finds its blooming application in civil engineering. One may be referred to the recent publications. For example, Adeli and coworkers (Karim and Adeli, 2003; Jiang and Adeli, 2004; Zhou and Adeli, 2003) applied the transform to traffic incident detection, traffic flow pattern analysis, and earthquake

*To whom correspondence should be addressed. E-mail: *cshuang@mail.nctu.edu.tw*.

record analysis, while Kim and Melhem (2004) studied damage detection.

Because of the successful application of wavelet transformation in data de-noising and data compression, Todorovska and Hao (2004) proposed storing the measured dynamic responses of a structure in a wavelet domain. In this case, it is natural to identify the modal parameters of a structure in a wavelet domain. Another advantage of performing the system identification in wavelet domain over performing it in a time domain is that the wavelet-based time–frequency decomposition of measured data provides the frequency components of data changing with time, which can give a rough estimation of natural frequencies. Wavelet transformations have been frequently applied to determine the dynamic characteristics of a time invariant linear system in the last decade. Schoenwald (1993) identified the parameters in the equation of motion for a system with a single degree of freedom by applying a continuous wavelet transform to the equation of motion. Ruzzene et al. (1997) applied a discrete wavelet transform and the Hilbert transform technique to determine the natural frequencies and damping of a structure system from its free vibration responses. Robertson et al. (1998a and 1998b) developed a procedure for extracting impulse response data from the dynamic responses of a structure and used an eigensystem realization algorithm to identify the dynamic characteristics of the structure. Gouttebroze and Lardies (2001) developed a wavelet identification approach in the time–frequency domain for elucidating the natural frequencies and damping of a structure from free vibration responses. Their approach cannot directly determine the mode shapes. Lardies and Gouttebroze (2002) further applied their wavelet identification technique (Gouttebroze and Lardies, 2001) to process the measured ambient vibrations of a TV tower, by first extracting a free vibration signal from the measured ambient vibration responses, using the conventional random decrement technique. Alvin et al. (2003) presented an overview of the use of the wavelet transformation technique for extracting impulse response functions; they also reviewed robust ways of identifying both proportional and nonproportional damping parameters.

The wavelet transform has also been further applied to system identification for a time-varying system or nonlinear system that has not been discussed in this article. Those who are interested in the topic may be referred to the recent literature on time-varying systems by Omenzetter et al. (2003) and Wei and Billings (2002) and on nonlinear systems by Ghanem and Romeo (2001) and Coca and Billings (2001).

These existing methodologies, involving wavelet transformation for identifying the dynamic characteristics of a linear structure, use the wavelet transformation either to extract impulse response functions or to determine natural frequencies and damping from free vibration responses. This article proposes a new procedure for applying a wavelet transformation to either the earthquake responses or the free vibration responses of a structure, to directly determine its natural frequencies, damping ratios, and mode shapes, without extracting impulse response functions. This procedure applies a discrete wavelet transformation to discrete equations of motion that closely resemble those in the time series ARX model. Then, the parameters of the equations of motion are determined by a least-squares approach, and are directly used to determine the dynamic characteristics of the structure. The proposed procedure is first validated using a numerical simulation of the earthquake responses of a six-story shear building. In this numerical experiment, the effects of noise and various mother functions in the wavelet transformation on the ability to identify the dynamic characteristics are also studied. Then, this procedure is further applied to the measured dynamic responses of a five-story steel frame in a shaking table test and to the dynamic responses of a five-span arch bridge in an impulse test, to demonstrate the feasibility of applying the proposed procedure to real data.

2 WAVELET TRANSFORMATION

It has been proved that functions in L^2 space, which is the functional space where a function $f(t)$ satisfies $\int_{-\infty}^{\infty} f^2(t)\,dt < \infty$, can be represented by their projections onto the space linearly spanned by a family of wavelet functions (Barbara, 1988). Let $\psi(t)$ be the so-called mother wavelet that must satisfy the admissibility condition

$$0 < C_\psi = \int_{-\infty}^{\infty} \frac{|\Psi(\omega)|}{\omega}\,d\omega < \infty \tag{1}$$

where $\Psi(\omega)$ is the Fourier transform of $\psi(t)$. The corresponding family of wavelets is generated by dilation and translation, and is denoted by

$$\psi_{a,b}(t) = a^{-1/2}\psi\left(\frac{t-b}{a}\right) \tag{2}$$

where a and b are dilation and translation parameters, respectively, and are real. The term a must be positive. Then, the wavelet transform of a function $f(t)$ in L^2 space is defined as

$$W_\psi f(a,b) = \langle f(t), \psi_{a,b}(t)\rangle = \int_{-\infty}^{\infty} f(t)\psi^*_{a,b}(t)\,dt \tag{3}$$

where $\langle\,,\rangle$ denotes inner product, and the superscript * stands for the complex conjugate. The inverse of the transformation is defined as

$$f(t) = \frac{1}{C_\psi}\int_{-\infty}^{\infty}\int_{-\infty}^{\infty} W_\psi f(a,b)\psi_{a,b}(t)\frac{1}{a^2}\,da\,db \tag{4}$$

To facilitate digital computation, the wavelet transform is normally transformed into a discrete form, in

which the family of wavelets is commonly expressed as

$$\psi_{m,n}(t) = 2^{-m/2}\psi(2^{-m}t - n) \tag{5}$$

where m and n are integers. Daubechies (1988) developed the conditions under which $\psi_{m,n}(t)$ forms an orthonormal basis, simplifying Equation (4) to

$$f(t) = \sum_m \sum_n \langle f(t), \psi_{m,n}(t)\rangle \psi_{m,n}(t) \tag{6}$$

where $\langle f(t), \psi_{m,n}(t)\rangle$ is the wavelet coefficient of $f(t)$ corresponding to $\psi_{m,n}(t)$.

Multiresolution analysis provides a formal approach to construct such an orthonormal basis (Mallat, 1989a and 1989b). In multiresolution analysis, the space V_0, to which the measured signal $f(t)$ belongs, is decomposed into as many subspaces as needed, and is expressed as

$$\begin{aligned} V_0 &= V_1 \oplus W_1 \\ &= V_2 \oplus W_2 \oplus W_1 \\ &= V_3 \oplus W_3 \oplus W_2 \oplus W_1 \\ &= \cdots \\ &= V_m \oplus W_m \oplus W_{m-1} \oplus \cdots \oplus W_2 \oplus W_1 \end{aligned} \tag{7}$$

where $\oplus$ denotes the union of two subspaces, V_i and W_j $(i,\ j = 1, 2, \ldots, m)$ are subspaces of V_0 and they satisfy the following properties, $V_m \subset V_{m-1}$, $V_m \perp W_m$ and $V_{m-1} = V_m \oplus W_m$. The intersection of any two of V_m, W_m, $W_{m-1}, \ldots,$ and W_1 is a null space. In each of the subspaces, V_m, W_m, $W_{m-1}, \ldots,$ and W_1, an orthonormal basis can be constructed as described in Mallat's articles (Mallat, 1989a and 1989b). Equation (5) with $n \in Z$ (the set of integers) can specify an orthonormal basis in W_m if the mother wavelet function $\psi(t)$ is properly chosen. An orthonormal basis in V_m is expressed as

$$\phi_{m,n}(t) = 2^{-m/2}\phi(2^{-m}t - n) \tag{8}$$

where $\phi(t)$ is called a scale function. The mother wavelet function must be related to the scale function to satisfy Equation (7) (Mallat, 1989a and 1989b). Because $\psi_{m,n}(t)$ and $\phi_{m,n}(t)$ are orthonormal bases in W_m and V_m, respectively, Equation (7) indicates the following orthonormal properties:

$$\langle \psi_{m,n}(t), \psi_{k,l}(t)\rangle = \begin{cases} 1 \text{ when } m = k \text{ and } n = l \\ 0 \qquad\qquad \text{elsewhere,} \end{cases} \tag{9a}$$

$$\langle \phi_{m,n}(t), \phi_{k,l}(t)\rangle = \begin{cases} 1 \text{ when } m = k \text{ and } n = l \\ 0 \qquad\qquad \text{elsewhere,} \end{cases} \tag{9b}$$

$$\langle \phi_{m,n}(t), \psi_{k,l}(t)\rangle = 0 \text{ for any } k,\ l,\ m,\ \text{and } n \tag{9c}$$

where k and l are also integers.

Hence, if the space V_0 is decomposed up to level j according to Equation (7), then $f(t)$ can be expressed in terms of orthonormal wavelets as

$$\begin{aligned} f(t) = &\sum_{m=1}^{j} \sum_{n\in Z} \langle f(t), \psi_{m,n}(t)\rangle \psi_{m,n}(t) \\ &+ \sum_{n\in Z} \langle f(t), \phi_{j,n}(t)\rangle \phi_{j,n}(t) \end{aligned} \tag{10}$$

Equation (10) can be easily established by using the commercial computer program MATLAB, in which a variety of families of wavelets are available.

3 MODAL IDENTIFICATION

The dynamic responses of a linear structure satisfy the equations of motion

$$[\mathbf{M}]\{\ddot{\mathbf{x}}\} + [\mathbf{C}]\{\dot{\mathbf{x}}\} + [\mathbf{K}]\{\mathbf{x}\} = \{\mathbf{f}\} \tag{11}$$

where $[\mathbf{M}]$, $[\mathbf{C}]$, and $[\mathbf{K}]$ are the mass, damping, and stiffness matrices of the structure system, respectively; $\{\ddot{\mathbf{x}}\}$, $\{\dot{\mathbf{x}}\}$, and $\{\mathbf{x}\}$ are the acceleration, velocity, and displacement response vectors of the system, and $\{\mathbf{f}\}$ is the input force vector. Usually, not all degrees of freedom of the system are measured in a field experiment, for economic reasons. Only some parts of $\{\ddot{\mathbf{x}}\}$ or $\{\dot{\mathbf{x}}\}$ are measured. Consequently, the measured response vector $\{\mathbf{y}\}$, which can be velocity or acceleration responses, satisfies the following discrete equation (Leuridan, 1984).

$$\{\mathbf{y}(t)\} = \sum_{i=1,2}^{I} [\Phi]_i \{\mathbf{y}(t-i)\} + \sum_{j=0,1}^{J} [\theta]_j \{\mathbf{f}(t-j)\} \tag{12}$$

where $\{\mathbf{y}(t-i)\}$ and $\{\mathbf{f}(t-i)\}$ are the measured responses and forces at time $t-i$, respectively, and $[\Phi]_i$ and $[\theta]_i$ are the parameter matrices to be determined. Equation (12) is very similar to the time series ARX model.

Performing a discrete wavelet transform on $\{\mathbf{y}(t-i)\}$ and $\{\mathbf{f}(t-j)\}$ with $i = 0, 1, 2, \ldots, I$ and $j = 0, 1, 2, \ldots, J$ yields

$$\begin{aligned} \{\mathbf{y}(t-i)\} = &\sum_{m=0}^{\bar{m}} \sum_{n=0}^{\bar{n}} \left\{\mathbf{y}^{(i)}(m,n)\right\} \psi_{m,n}(t) \\ &+ \sum_{n=0}^{\bar{n}} \left\{\hat{\mathbf{y}}^{(i)}(\bar{m},n)\right\} \phi_{\bar{m},n}(t) \end{aligned} \tag{13a}$$

$$\begin{aligned} \{\mathbf{f}(t-j)\} = &\sum_{m=0}^{\bar{m}} \sum_{n=0}^{\bar{n}} \left\{\mathbf{f}^{(j)}(m,n)\right\} \psi_{m,n}(t) \\ &+ \sum_{n=0}^{\bar{n}} \left\{\hat{\mathbf{f}}^{(j)}(\bar{m},n)\right\} \phi_{\bar{m},n}(t) \end{aligned} \tag{13b}$$

Notably, for finite measured responses and input forces, $\bar{n}$ depends on m. Substituting Equations (13a) and (13b) into Equation (12), performing the inner product with respect to $\psi_{m,n}(t)$ on both sides of the resulting equation,

and applying the orthonormal properties specified by Equations (9a) and (9b) yields

$$\{\mathbf{y}^{(0)}(m,n)\} = \sum_{i=1}^{I} [\mathbf{\Phi}]_i \{\mathbf{y}^{(i)}(m,n)\} + \sum_{j=0}^{J} [\boldsymbol{\theta}]_j \{\mathbf{f}^{(j)}(m,n)\} \tag{14}$$

Similarly, carrying out the inner product with respect to $\phi_{\bar{m},n}(t)$, instead of $\psi_{m,n}(t)$, in the process of obtaining Equation (14) from Equations (12), (13a), and (13b) leads to

$$\{\hat{\mathbf{y}}^{(0)}(\bar{m},n)\} = \sum_{i=1}^{I} [\mathbf{\Phi}]_i \{\hat{\mathbf{y}}^{(i)}(\bar{m},n)\} + \sum_{j=0}^{J} [\boldsymbol{\theta}]_j \{\hat{\mathbf{f}}^{(j)}(\bar{m},n)\} \tag{15}$$

Rearranging Equations (14) and (15) for different values of m and n yields

$$[\mathbf{Y}^{(0)}] = [\mathbf{C}] \begin{bmatrix} [\mathbf{Y}] \\ [\mathbf{F}] \end{bmatrix} \tag{16}$$

where

$$[\mathbf{C}] = \begin{bmatrix} [\mathbf{\Phi}]_1 & [\mathbf{\Phi}]_2 & \cdots & [\mathbf{\Phi}]_I & [\boldsymbol{\theta}]_0 & [\boldsymbol{\theta}]_1 & \cdots & [\boldsymbol{\theta}]_J \end{bmatrix} \tag{17a}$$

$$[\mathbf{Y}] = \begin{bmatrix} [\mathbf{Y}^{(1)}]^T & [\mathbf{Y}^{(2)}]^T & \cdots & [\mathbf{Y}^{(I)}]^T \end{bmatrix}^T \tag{17b}$$

$$[\mathbf{F}] = \begin{bmatrix} [\mathbf{F}^{(0)}]^T & [\mathbf{F}^{(1)}]^T & \cdots & [\mathbf{F}^{(J)}]^T \end{bmatrix}^T \tag{17c}$$

$$[\mathbf{Y}^{(i)}] = \begin{bmatrix} \{\mathbf{y}^{(i)}(1,1)\} & \{\mathbf{y}^{(i)}(1,2)\} & \cdots & \{\mathbf{y}^{(i)}(\bar{m},\bar{n})\} & \{\hat{\mathbf{y}}^{(i)}(\bar{m},1)\} & \{\hat{\mathbf{y}}^{(i)}(\bar{m},2)\} & \cdots & \{\hat{\mathbf{y}}^{(i)}(\bar{m},\bar{n})\} \end{bmatrix} \tag{17d}$$

$$[\mathbf{F}^{(i)}] = \begin{bmatrix} \{\mathbf{f}^{(i)}(1,1)\} & \{\mathbf{f}^{(i)}(1,2)\} & \cdots & \{\mathbf{f}^{(i)}(\bar{m},\bar{n})\} & \{\hat{\mathbf{f}}^{(i)}(\bar{m},1)\} & \{\hat{\mathbf{f}}^{(i)}(\bar{m},2)\} & \cdots & \{\hat{\mathbf{f}}^{(i)}(\bar{m},\bar{n})\} \end{bmatrix} \tag{17e}$$

Typically, Equation (16) represents a set of overdetermined linear algebraic equations. The solution for the matrix of parameters $[\mathbf{C}]$ is determined by a conventional least-squares approach:

$$[\mathbf{C}] = [\mathbf{Y}^{(0)}] \begin{bmatrix} [\mathbf{Y}] \\ [\mathbf{F}] \end{bmatrix}^T \left(\begin{bmatrix} [\mathbf{Y}] \\ [\mathbf{F}] \end{bmatrix} \begin{bmatrix} [\mathbf{Y}] \\ [\mathbf{F}] \end{bmatrix}^T \right)^{-1} \tag{18}$$

Equation (12) reveals that the modal parameters of a structure are determined from $[\mathbf{\Phi}]_i$ with $i = 1, 2, \ldots, I$. A matrix $[\mathbf{G}]$ is constructed from $[\mathbf{\Phi}]_i$ as

$$[\mathbf{G}] = \begin{bmatrix} \mathbf{0} & \mathbf{I} & \mathbf{0} & \mathbf{0} & \cdots & \mathbf{0} \\ \mathbf{0} & \mathbf{0} & \mathbf{I} & \mathbf{0} & \cdots & \mathbf{0} \\ \vdots & \vdots & \vdots & \vdots & \vdots & \vdots \\ \mathbf{0} & \mathbf{0} & \mathbf{0} & \mathbf{0} & \cdots & \mathbf{I} \\ [\mathbf{\Phi}]_I & [\mathbf{\Phi}]_{I-1} & & \cdots & & [\mathbf{\Phi}]_1 \end{bmatrix} \tag{19}$$

The dynamic characteristics of the structure are determined from the eigenvalues and eigenvectors of $[\mathbf{G}]$ (Huang, 1999). Let λ_k be the kth eigenvalue of $[\mathbf{G}]$, and let $\{\tilde{\psi}_k\}$ be the corresponding eigenvector. Furthermore, express $\{\tilde{\psi}_k\}^T$ as $(\{\tilde{\psi}_k\}_1^T \{\tilde{\psi}_k\}_2^T \cdots \{\tilde{\psi}_k\}_n^T)$ with each $\{\tilde{\psi}_k\}_i$ having the same number of components as $\{\mathbf{y}\}$ has. Because $\{\tilde{\psi}_k\}_i = \gamma_{ij}\{\tilde{\psi}_k\}_j$ where $\gamma_{ij}$is a scalar (Huang, 1999), these vectors $(\{\tilde{\psi}_k\}_i, i = 1, 2, \ldots, n)$ correspond to a mode shape of the structural system.

The eigenvalue λ_k is typically a complex number, set equal to $a_k + ib_k$. The frequency and damping ratio of the system are computed by

$$\tilde{\beta}_k = \sqrt{\alpha_k^2 + \beta_k^2} \tag{20a}$$

$$\xi_k = -\alpha_k / \tilde{\beta}_k \tag{20b}$$

where

$$\beta_k = \frac{1}{\Delta t} \tan^{-1}\left(\frac{b_k}{a_k}\right) \tag{21a}$$

$$\alpha_k = \frac{1}{2\Delta t} \ln\left(a_k^2 + b_k^2\right) \tag{21b}$$

Here, Δt is the inverse of the sampling rate of the measurement, $\tilde{\beta}_k$ is the pseudo-undamped circular natural frequency and ξ_k is the modal damping ratio.

4 VERIFICATION

A numerical simulation was undertaken for a six-story shear building subjected to a base excitation, to validate the proposed procedure. The simulation was run for a modal damping ratio of 5%. The theoretical natural frequencies of the system were 0.801, 2.14, 3.15, 4.25, 5.04, and 5.37 Hz. The acceleration responses of the six degrees of freedom, some of which are depicted in Figure 1, were used in the following data processing. The data were sampled at 250 Hz.

The modal assurance criterion (MAC) (Allemang and Brown, 1983), which is a correction-type indicator, was applied to check for agreement between the identified mode shapes and the theoretical ones:

$$\mathrm{MAC}(\{\varphi_{iI}\}, \{\varphi_{iA}\}) = \frac{\left|\{\varphi_{iI}\}^T \{\varphi_{iA}\}\right|^2}{\{\varphi_{iI}\}^T \{\varphi_{iI}\} \{\varphi_{iA}\}^T \{\varphi_{iA}\}} \tag{22}$$

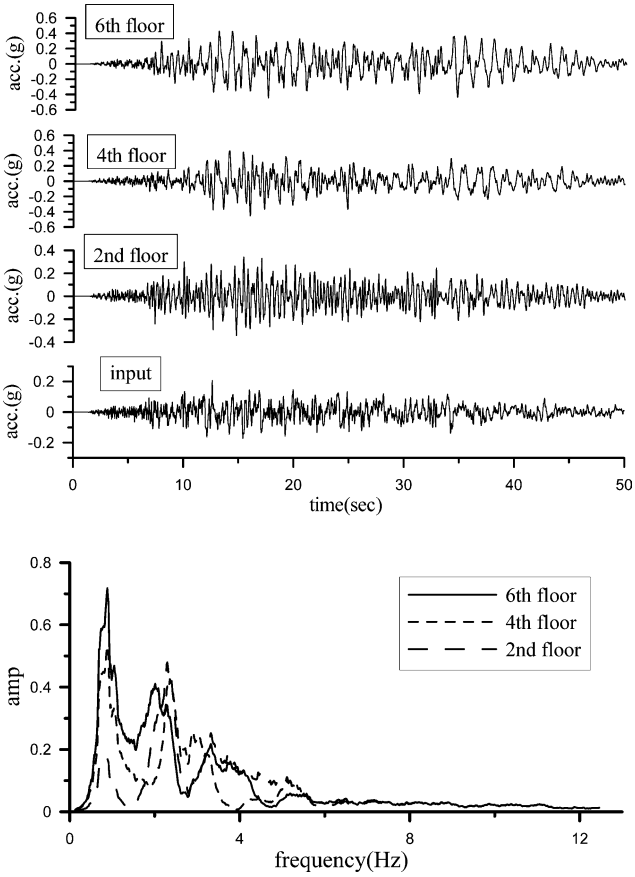

Fig. 1. Simulated responses of a six-story shear building and the corresponding Fourier spectra.

where $\{\varphi_{iI}\}$ is the identified ith mode shape and $\{\varphi_{iA}\}$ is the corresponding analytical mode shape. The value of MAC is between zero and unity. When two mode shapes are more similar, MAC is closer to one. When two mode shapes are orthogonal to each other, MAC is zero.

Notably, in the following numerical studies, the identified results are referred to as "accurate" if the differences between the identified frequencies and modal damping ratios and the theoretical ones are under 2% and 20%, respectively, and if the MAC values exceed 0.9. These numbers in this criterion for accurate results are empirically selected. Because the values of damping ratios are normally in a very small range, a relative large tolerance for the error in identifying damping ratios is used in the criterion. Numerical studies were also performed to elucidate the effects of mother wavelet functions and noise on the identified results. The signals were decomposed into the sixth level ($\bar{m} = 6$) in Equation (7), using orthonormal wavelets. The results are presented for $I = J$ in Equation (12).

4.1 Effects of mother wavelet functions

Three different mother functions—"sym1," "sym4," and "sym10" shown in Figure 2—were used to generate different sets of wavelet functions and to process the acceleration responses of the second, fourth, and sixth stories and the input excitation. The theoretical background of the development of these mother functions can be found in Daubechies (1992). The data at $t = 8$–10 seconds in Figure 1 were processed. Figure 3 plots the results obtained using different values of I and J in Equation (12) and different mother functions. Using the wavelets generated by the mother functions "sym1" or "sym10" along with the values of I and J larger than 20 gives accurate identified results. Using the mother function "sym4" along with using the values of I and J larger than 25 also yields accurate results. These results reveal that, although the mother function may somewhat affect the identified results, different mother functions eventually

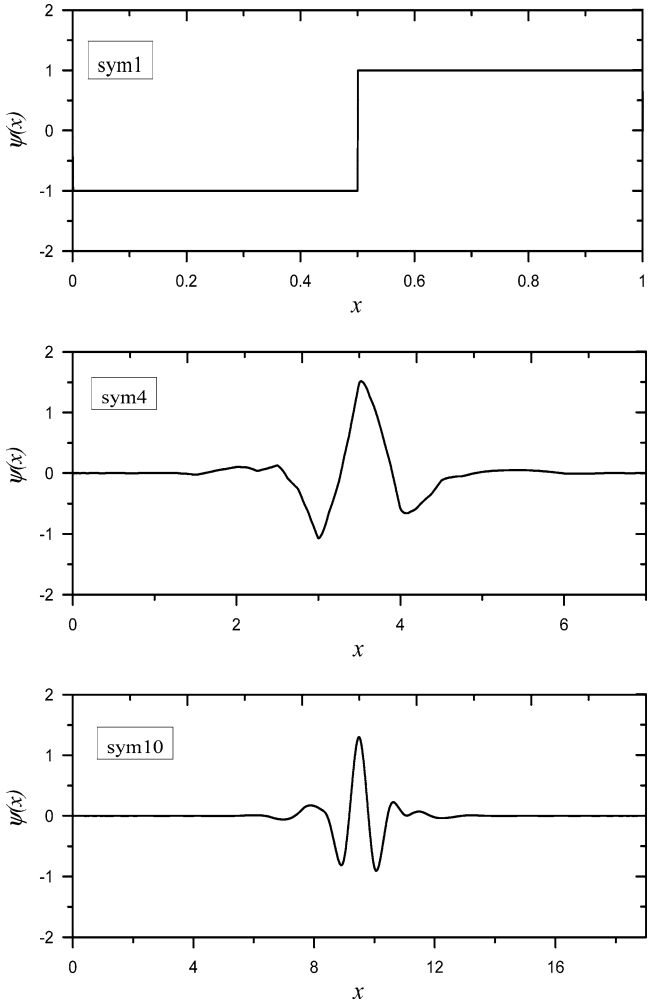

Fig. 2. Wavelet functions of sym1, sym4, and sym10.

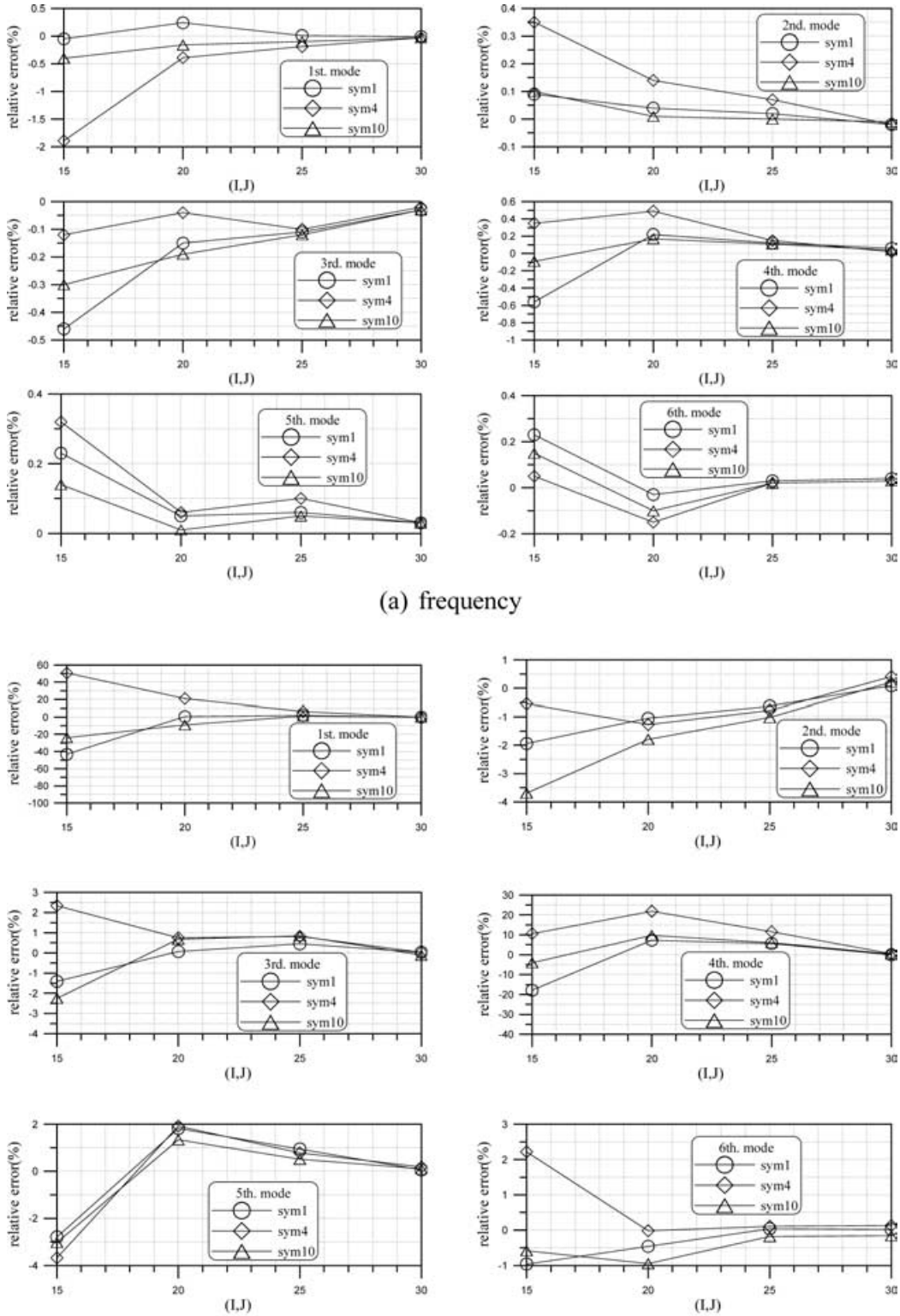

Fig. 3. Identified results obtained using responses of three floors.

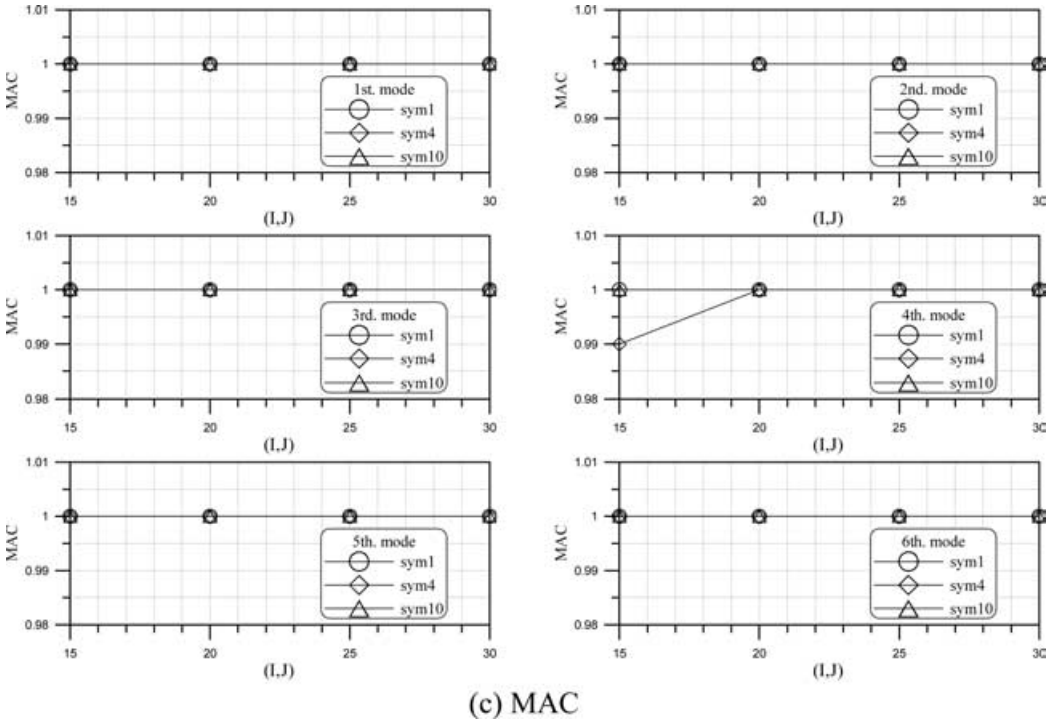

(c) MAC

Fig. 3. (Continued).

result in satisfactory identified results if the values of I and J are sufficiently large.

Notably, Figure 3 also shows that, as the values of I and J in Equation (12) increase, the identified frequencies converge faster than the identified modal damping ratios. As I and J increase, other than structural modes, extra spurious modes arise and computational effort also increases. Nevertheless, the desired structural modes consistently occur when the values of I and J are large enough and continue to increase.

4.2 Effects of noise

In real applications, measured responses always contain some level of corrupting noise. Noise, yielding a 10% variance of the signal-to-noise ratio, was randomly added to the computed responses and input excitation to simulate this situation. Figure 4 plots the results obtained from processing the noisy input and acceleration responses of all six stories by using various values of I and J and the mother functions. The responses at $t = 8$–16 seconds were used in this analysis. Figure 4 reveals that larger values of I and J are required to yield accurate results from noisy data than are required for yielding such results from non-noisy data. The mother function "sym4" somewhat outperforms "sym1" and "sym10." When $I = J = 53$, "sym4" yields accurate results but "sym1" and "sym10" do not. To reach accurate results "sym1" and "sym10" need slightly larger values of I and J.

Figures 3 and 4 validate the proposed procedure for accurately identifying dynamic characteristics from the observed responses, even when the responses include noise. The dynamic characteristics of a structure are consistently identified with very high accuracy when the values of I and J are large enough. Furthermore, as long as the values of I and J are sufficiently high, different mother functions seem to affect the identified results insignificantly. Notably, when dealing with noisy data with more than 10% variance of the signal-to-noise ratio, one may need to either use larger values of I and J or apply some de-noising techniques to eliminate the noise.

5 APPLICATION TO REAL DATA

The preceding section demonstrated the feasibility of the proposed procedure by processing simulated data. This section further applies this procedure to data measured in the laboratory or in the field. The dynamic responses of steel frames from shaking table tests and the free vibration responses of an arch bridge from impulsive tests were analyzed. Mother function "sym4" was applied in these analyses.

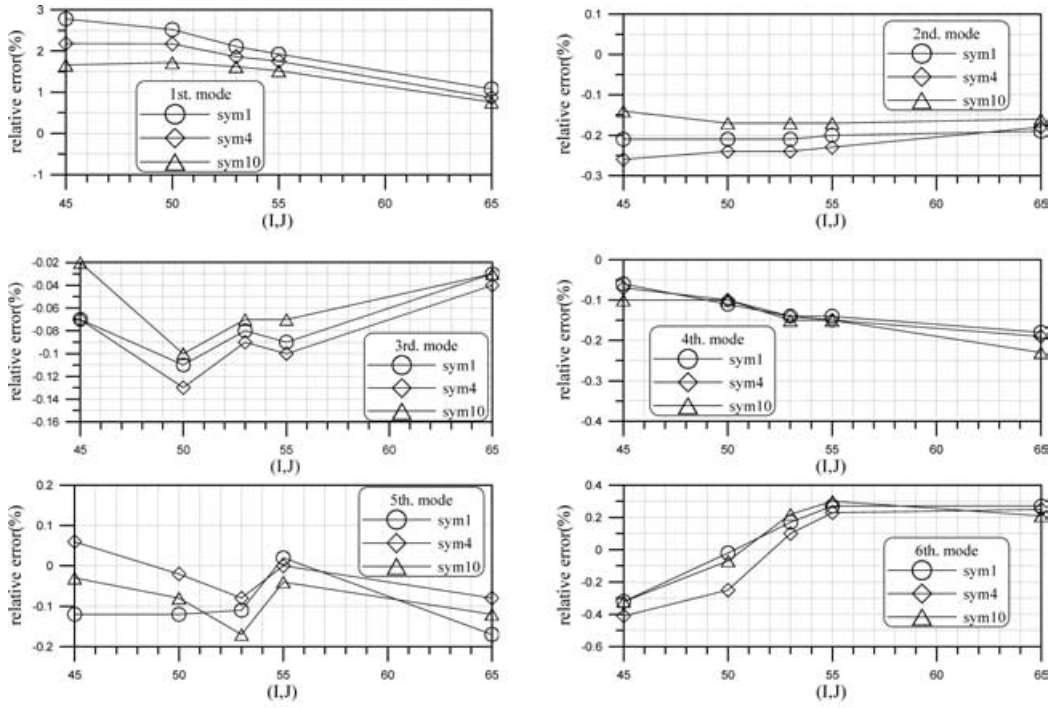

(a) frequency

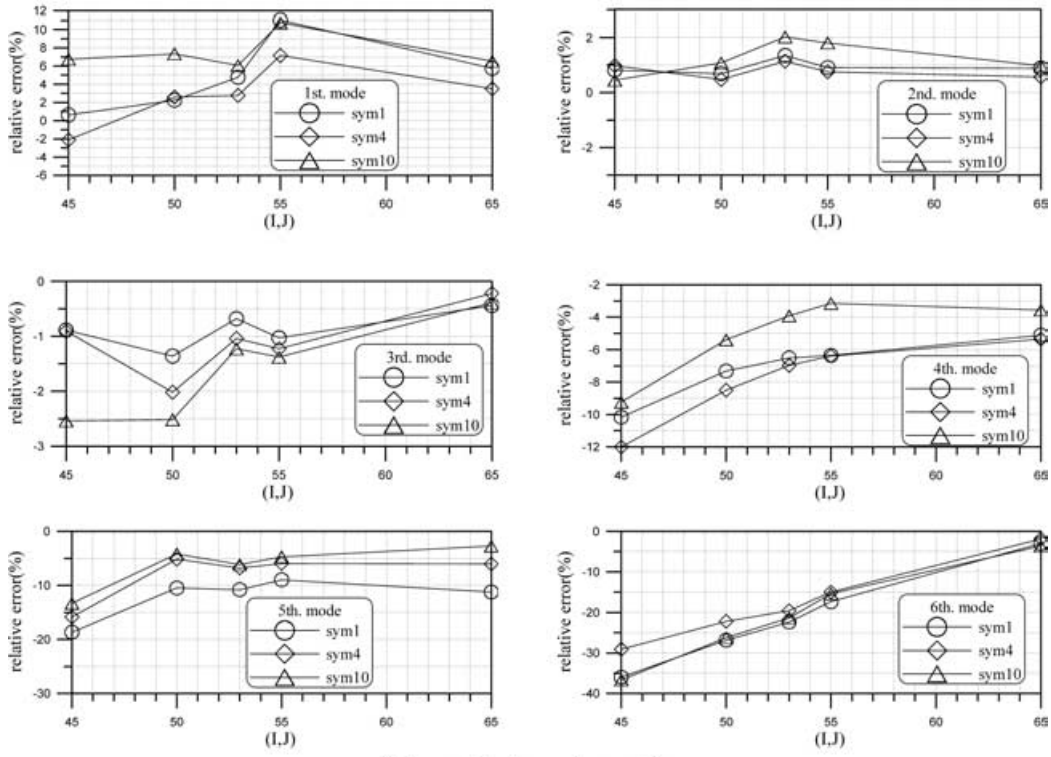

(b) modal damping ratio

Fig. 4. Effects of noise on identified results.

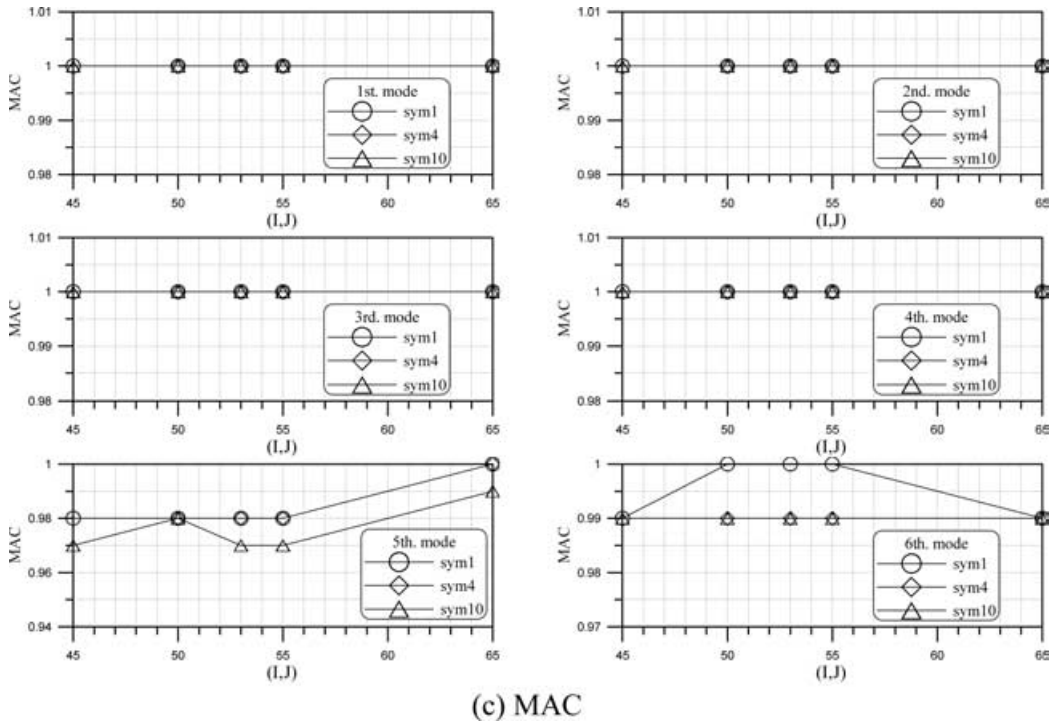

(c) MAC

Fig. 4. (Continued).

5.1 Application to dynamic responses from shaking table tests

The shaking table test is a popular and sophisticated test used in the laboratory to study the behaviors of structures under earthquake. The National Center for Research on Earthquake Engineering in Taiwan conducted a series of shaking table tests on three steel frames (Yeh et al., 1999) (Figures 5 and 6). One frame, denoted as "std," was 3 m long, 2 m wide, and 6.5 m high. Lead blocks were piled on each floor such that the mass of each floor was approximately 3664 kg. This frame is structurally regular. The second frame, which is structurally irregular with respect to mass and denoted as "add_m," was identical to "std" except in that extra lead blocks were placed on the fourth floor such that the floor was 25% heavier than that in "std." The third frame, which is structurally irregular with respect to stiffness and denoted as "add_k," was identical to "std" except in that stiffening braces were incorporated into the fourth story. These frames were subjected to base excitations specified by records of real earthquakes, such as the Kobe earthquake, but with different multiplicative factors applied. The responses were sampled at 1000 Hz. Figure 7 depicts the acceleration responses of the second and fourth floors in the long-span direction for frame "add_k," subjected to 8% of the Kobe earthquake.

Table 1 summarizes the identified dynamic characteristics of the three frames obtained using the acceleration responses of all floors and the input excitation in the long-span direction. The results were obtained from the responses of all floors at $t = 7$–20 seconds. The responses were reproduced with a 200-Hz sampling rate, using one data point out of every five raw data points, to reduce computational time and to match to the typical sampling rate used during the monitoring of responses of a structure under earthquake in the field. Frames "std" and "add_k" were subjected to 8% of the Kobe earthquake, while "add_m" was subjected to 10% of the Kobe earthquake motion.

In Table 1, the MAC values for the frame "std" indicate excellent agreement between the identified mode shapes and the analytical mode shapes obtained using the finite element package, DRAIN_2D. Figure 8 also displays this consistency between the identified and the analytical mode shapes. The MAC values for frames "add_k" and "add_m" reveal the correlation between the mode shapes of these two frames and the mode shapes of frame "std." These MAC values and the mode shapes shown in Figure 8 imply that placing the extra weight on the fourth floor did not significantly alter the mode shapes,

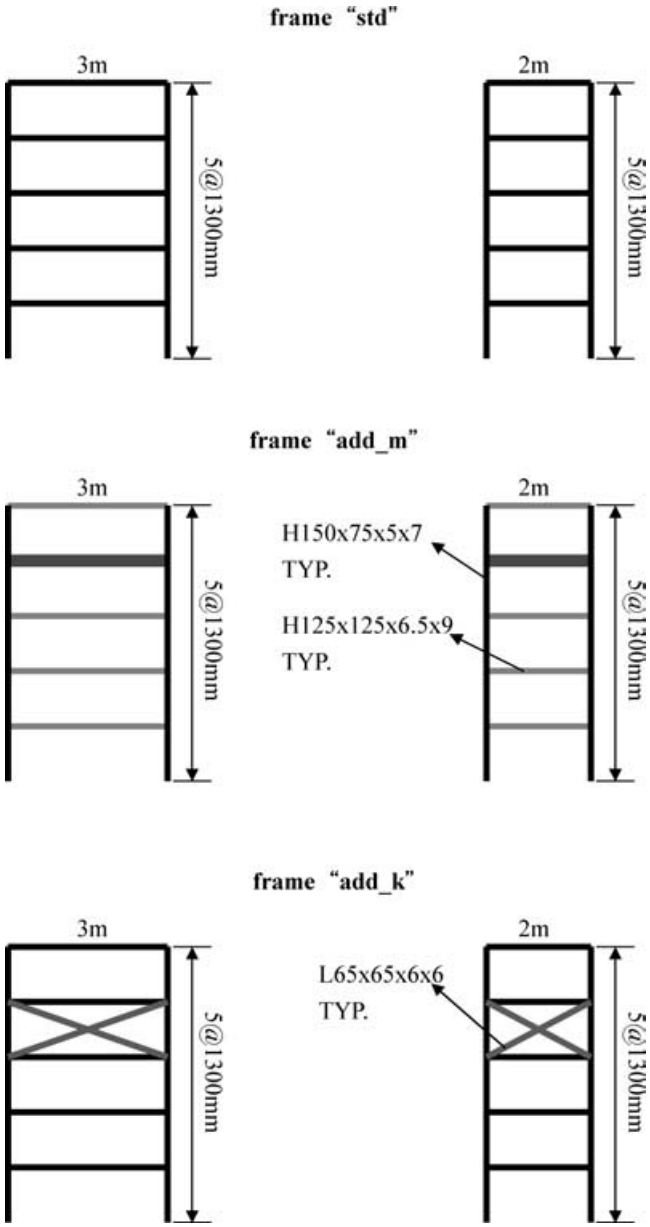

Fig. 5. Simple sketch of three five-story frames.

whereas incorporating the stiffening braces in the fourth story did substantially impact the fourth and fifth mode shapes.

As expected, the identified frequencies of frame "std" are slightly larger than those of frame "add_m," and generally smaller than those of frame "add_k." Notably, the frequency of the third mode of frame "add_k" is almost identical to that of frame "std," because the modal components at the third and fourth floors in this mode of frame "add_k" are almost identical, and so the braces between these two floors had no effect in this particular mode.

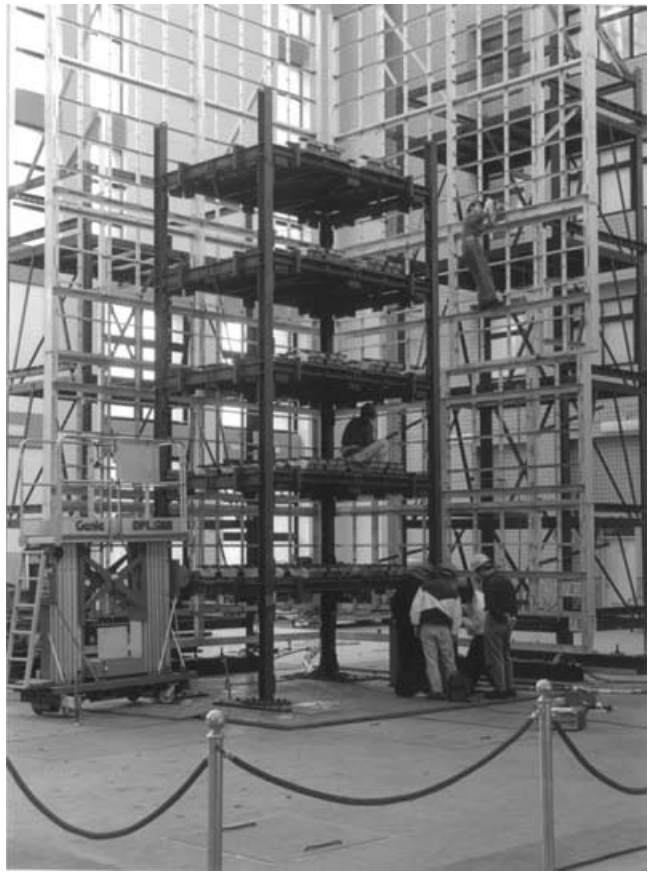

Fig. 6. A photo of frame "std" on shaking table.

The identified modal damping ratios for different frames are smaller than 2%, especially in higher modes. In the design process, a 2% modal damping is typically used in the dynamic analysis of a steel structure.

Table 1 also lists the results obtained using a subspace approach (Huang and Lin, 2001). The present results generally display excellent agreement with those in Huang and Lin (2001). However, the fifth mode of frame "add_k" was identified by the approach described herein, but not by the subspace approach, even though the fifth mode was not significantly excited because the high-frequency components of the input were too weak (Figure 7). Notably, the frequency of the fifth mode determined using the presented approach is consistent with that reported in Huang and Lin (2001), obtained by processing the responses to a white noise input.

5.2 Application to impulse tests of an arch bridge

Impulse tests were conducted on a five-span arch prestressed concrete bridge with a total length of 440 m (Yang et al., 2000) (Figure 9). The deck of the bridge was around 22.5 m wide and 35 m above the ground.

Table 1
Comparison of identified modal parameters for different frames

Frame input method		*std Kobe 8%*		*add_k Kobe 8%*		*add_m Kobe 10% present*
		Subspace (Huang and Lin, 2001)	*Present*	*Subspace (Huang and Lin, 2001)*	*Present*	
Frequency (Hz)	1	1.40	1.40	1.52	1.52	1.34
	2	4.53	4.53	5.94	5.94	4.52
	3	8.23	8.24	8.22	8.22	8.06
	4	12.39	12.39	14.00	13.99	11.93
	5	15.99	15.99	/	18.29	15.75
Damping (%)	1	1.30	1.54	1.90	1.78	1.41
	2	0.16	0.18	0.17	0.20	0.20
	3	0.19	0.18	0.18	0.17	0.20
	4	0.13	0.13	0.18	0.13	0.16
	5	0.10	0.10	/	0.97	0.12
MAC	1	1.00	1.00	0.99	0.99	1.00
	2	1.00	1.00	0.91	0.90	1.00
	3	1.00	1.00	1.00	0.99	0.99
	4	1.00	1.00	0.65	0.63	0.99
	5	1.00	1.00	/	0.78	0.99

Note: / denotes no data available.

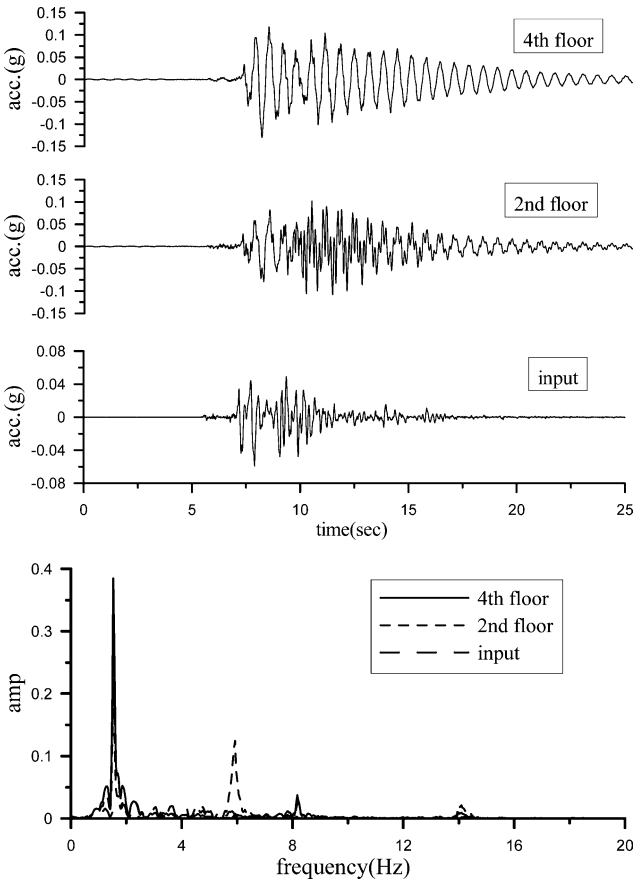

Fig. 7. Responses of frame "add_k" and the corresponding Fourier spectra.

The bridge was supported by rollers in the longitudinal direction, but was constrained in the transverse and vertical directions at both ends, which were separated from the adjacent spans by expansion joints. The transverse impulsive force was generated by suddenly braking a loaded truck that weighed about 15 tons and was traveling in a direction with an inclined angle of 30° from the centerline of the deck.

The transverse velocity responses of the bridge were measured by highly sensitive sensors of the servo velocity type. The number of sensors available was limited, so the bridge was divided into four segments, as illustrated in Figure 9. In each segment, the sensors were positioned at 20-m intervals along the centerline of the bridge deck. The free vibration responses in each of the four segments subjected to an impulsive force were measured consecutively. The overlapping observation stations in any two adjacent segments were used to correlate the mode shapes identified from the responses in different segments.

Figure 10 depicts typical responses observed at stations in different segments. The recorded responses contain some contributions from the ambient vibration that cannot be separated from the free vibration responses. To eliminate the influence of ambient vibration, the recorded responses within 8 seconds after the maximum response occurred were employed in the identification analysis. The responses in the different segments were separately processed. Table 2 summarizes the identified natural frequencies and corresponding damping ratios. Some of the identified natural frequencies in Table 2

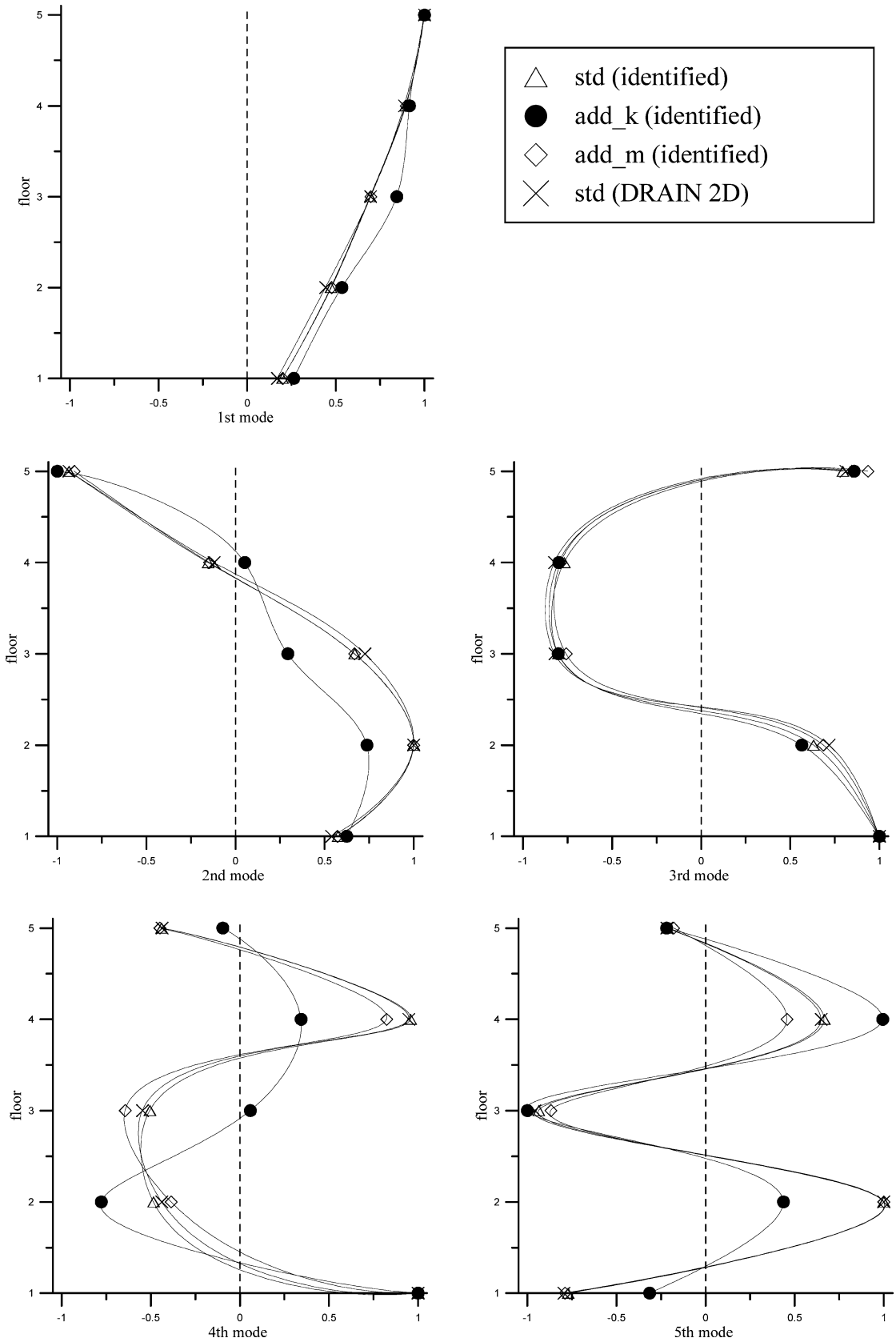

Fig. 8. Mode shape for three steel frames.

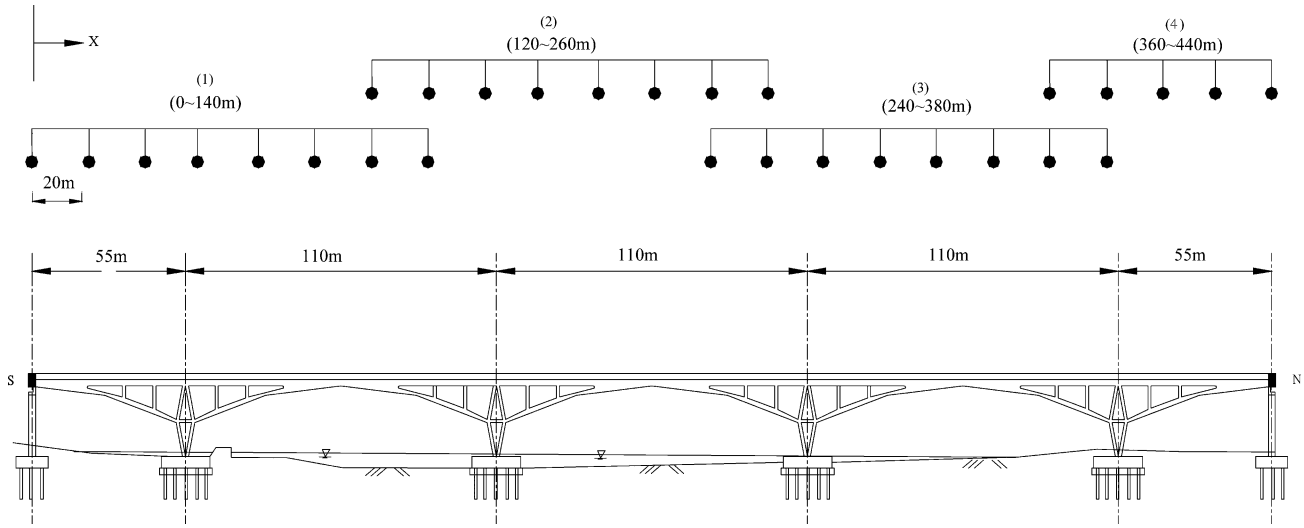

Fig. 9. A sketch of the five-span arch bridge and sensor layout for impulsive tests.

correspond very well to those associated with the peaks of the Fourier spectra displayed in Figure 10. Figure 11 presents the identified mode shapes. Nine modes were identified with frequencies of less than 5 Hz.

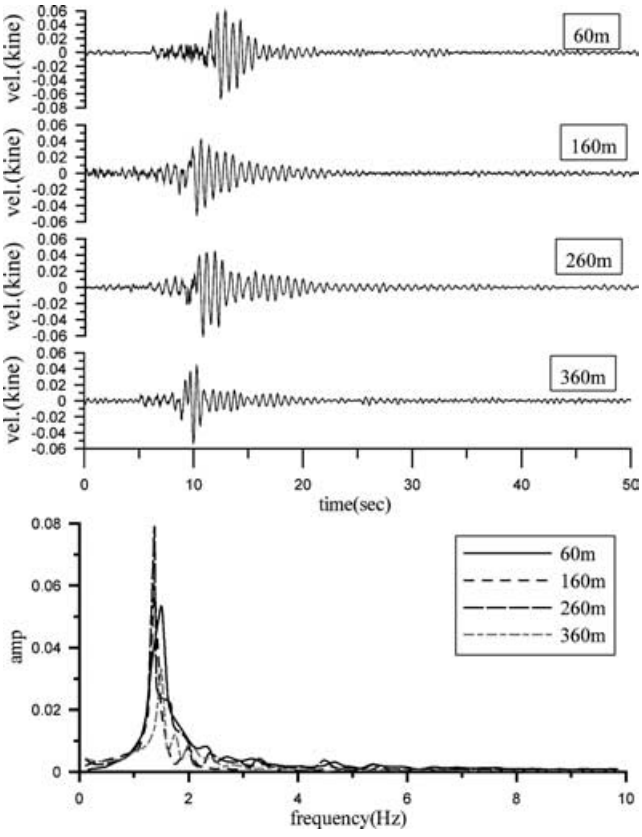

Fig. 10. Impact responses at different stations and the corresponding Fourier spectra.

Figure 11 also depicts the mode shapes obtained from finite element analysis (Yang et al., 2000) and similar to the identified mode shapes. The legend also states the corresponding frequencies. The finite element model was established according to the designed geometry of the bridge and the material properties. Comparing the finite element results with the measured results indicates the finite element model is inadequate. The finite element model significantly underestimates the frequencies and also totally misses some modes. Apparently, the finite element model used in the structure design needs further refinement, through a more realistic evaluation of the boundary conditions, geometric and material properties of the bridge (that is, the constants for soil springs, the real Young's modulus, the nonuniform cross-section of girders and arches) by experiments or by model updating techniques, a task that is beyond the scope of the present work.

Table 2
Identified results from impulse tests

Mode	*f (Hz)*	*Damping (%)*
1	1.37	2.47
2	1.48	3.26
3	1.73	4.13
4	2.00	3.57
5	2.29	2.59
6	3.05	3.82
7	3.50	3.62
8	4.40	1.60
9	4.61	2.78

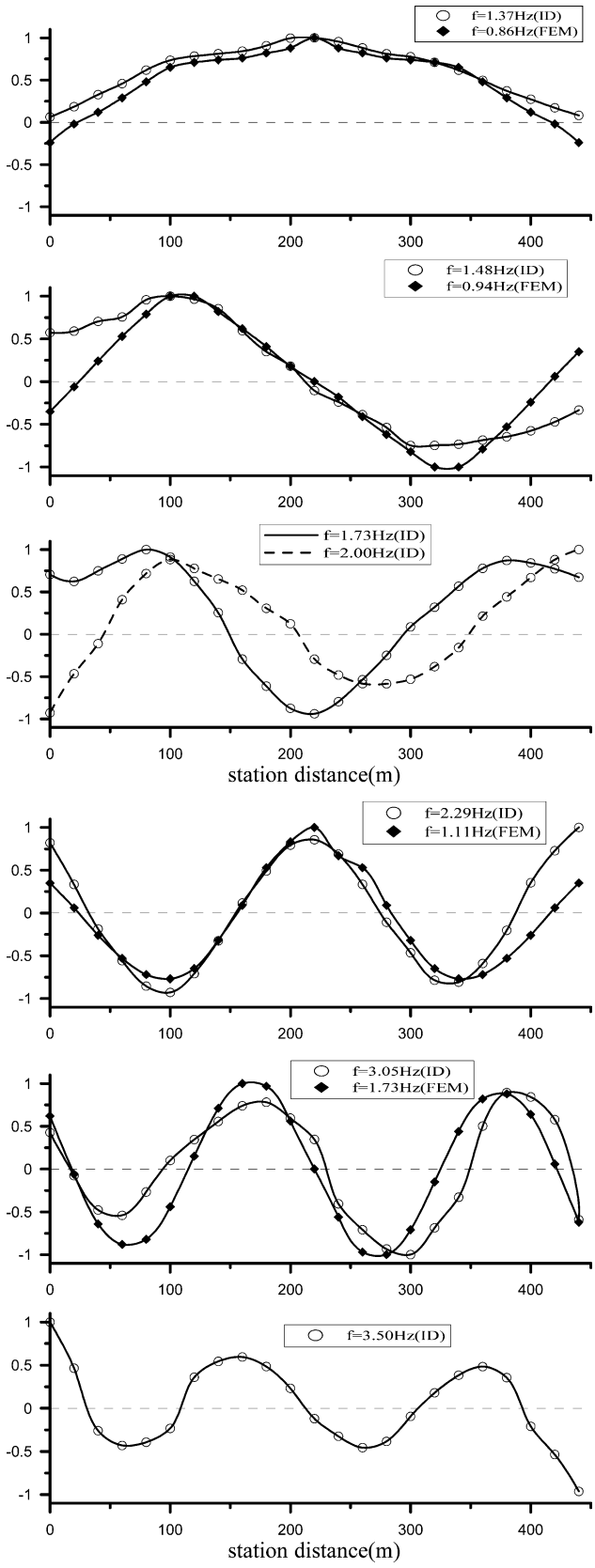

Fig. 11. Comparison of identified mode shapes with finite element results.

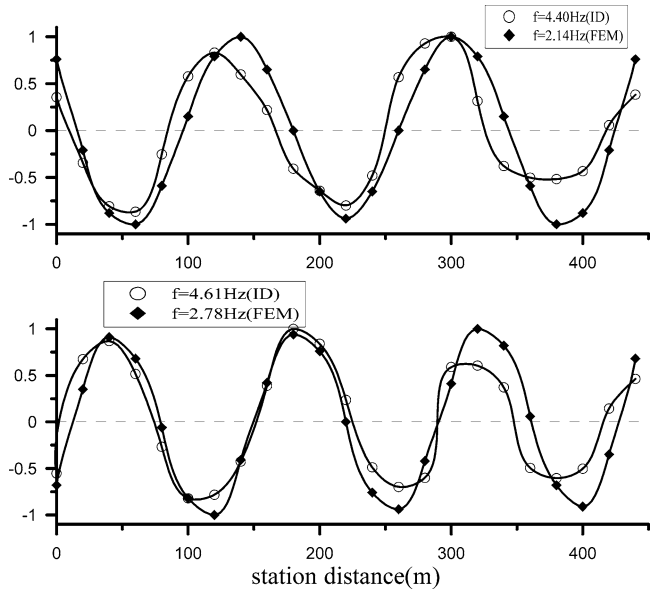

Fig. 11. (Continued).

6 CONCLUDING REMARKS

This article presented a wavelet-based approach for identifying the dynamic characteristics of a structure from its seismic responses or free vibration responses. A discrete wavelet transformation was applied to the measured responses, using an orthonormal wavelet basis. Consequently, the discrete equations of motion were reconstructed in various wavelet subspaces. The coefficients in the discrete equations of motion were determined by a conventional least-squares approach. Then, the natural frequencies, damping ratios, and mode shapes of the structure were calculated from these coefficients.

Numerically simulated responses of a six-story shear building under earthquake were used to validate the proposed approach. The effects of the wavelet mother functions and of noise on the ability to identify the dynamic characteristics were also investigated. The proposed approach did provide accurate results, even for noisy data. The wavelet mother functions did not significantly influence the identified results when the values of I and J in Equation (12) were large.

The proposed approach was also applied to process measured responses of three five-story steel frames in shaking table tests and to responses of a five-span arch bridge in impulse tests. The present results for steel frames are in good agreement with published results obtained from a subspace approach. However, the proposed approach identified a higher mode that the subspace approach failed to identify because this mode was not significantly excited, indicating the superiority of the proposed approach over the subspace approach. Nine

modes with frequencies of less than 5 Hz were identified from the transverse responses of the five-span arch bridge. The identified results differ markedly from those of the finite element analysis, implying the need for updating the finite element model.

ACKNOWLEDGMENTS

The research reported herein was sponsored by the National Science Council, R.O.C. (NSC 93-2625-Z-009-006) and the Central Weather Bureau, Ministry of Transportation and Communications (MOTC-CWB-92-E-11), which are gratefully acknowledged. The appreciation is also extended to the National Center for Research on Earthquake Engineering for providing shaking table test data.

REFERENCES

Allemang, R. L. & Brown, D. L. (1983), A correlation coefficient for modal vector analysis, in *Proceeding of the First International Modal Analysis Conference*, Bethel, Connecticut, U.S.A., pp. 110–16.

Alvin, K. F., Robertson, A. N., Reich, G. W. & Park, K. C. (2003), Structural system identification: From reality to models, *Computers and Structures*, **81**(12), 1149–76.

Barbara, B. H. (1996), *The World According to Wavelets*, A. K. Peters Ltd., Wellesley, MA.

Brown, D., Allemang, R., Zimmerman, R. & Mergeay, M. (1979), Parameter estimation techniques for modal analysis, *SAE Transaction*, **88**(1), 828–46.

Coca, D. & Billings, S. A. (2001), Non-linear system identification using wavelet multiresolution models, *International Journal of Control*, **74**(18), 1718–36.

Combes, J. M., Grossmann, A. & Tchamitchian, P. H. (1990), *Wavelet: Time-Frequency Methods and Phase Space*, Springer-Verlag, Berlin.

Daubechies, I. (1988), Orthonormal basis of compactly supported wavelets, *Communication for Pure & Applied Mathematics*, **41**, 909–96.

Daubechies, I. (1992), *Ten Lectures on Wavelets*, Society for Industrial and Applied Mathematics, Philadelphia, Pennsylvania.

Flandrin, P. (1990), Wavelets and related time-scale transforms, *SPIE Advanced Signal-Processing Algorithms, Architectures, and Implementation*, **1348**, 2–13.

Ghanem, R. & Romeo, F. (2001), Wavelet-based approach for model and parameter identification of non-linear systems, *International Journal of Non-Linear Mechanics*, **36**(5), 835–59.

Gouttebroze, S. & Lardies, J. (2001), On using the wavelet transform in modal analysis, *Mechanics Research Communications*, **28**(5), 561–9.

Huang, C. S. (1999), *A Study on Techniques for Analyzing Ambient Vibration Measurement (II)—Time Series Methods*, Rep. No. NCREE-99-018, National Center for Research on Earthquake Engineering, Taipei, Taiwan (in Chinese).

Huang, C. S. & Lin, H. L. (2001), Modal identification of structures from ambient vibration, free vibration, and seismic response data via a subspace approach, *Earthquake Engineering and Structural Dynamics*, **30**(12), 1857–78.

Ibrahim, S. R. & Mikulcik, E. C. (1977), A method for direct identification of vibration parameters from the free responses, *Bulletin of Shock and Vibration*, **47**(4), 183–98.

Jawerth, B. & Sweldens, W. (1994), Overview of wavelet based multiresolution analyses, *SIAM Review*, **36**(3), 377–412.

Jiang, X. & Adeli, H. (2004), Wavelet packet-autocorrelation function method for traffic flow pattern analysis, *Computer-Aided Civil and Infrastructure Engineering*, **19**(5), 324–37.

Karim, A. & Adeli, H. (2003), Fast automatic incident detection on urban and rural freeways using the wavelet energy algorithm, *Journal of Transportation Engineering, ASCE*, **129**(1), 57–68.

Kim, H. & Melhem, H. (2004), Damage detection of structures by wavelet analysis, *Engineering Structures*, **26**(3), 347–62.

Kobayashi, M. (2001), Wavelets and their applications in industry, *Nonlinear Analysis, Theory, Methods and Applications*, **47**(3), 1749–60.

Lardies, J. & Gouttebroze, S. (2002), Identification of modal parameters using the wavelet transform, *International Journal of Mechanical Sciences*, **44**(11), 2263–83.

Leuridan, J. M. (1984), Some direct parameters model identification methods applicable for multiple input modal analysis, Ph.D. dissertation, Department of Mechanical and Industrial Engineering, University of Cincinnati, USA.

Loh, C. H. & Lin, H. M. (1996), Application of off-line and on-line identification techniques to building seismic response data, *Earthquake Engineering and Structural Dynamics*, **25**(3), 269–90.

Mallat, S. (1989a), Multiresolution approach to wavelets in computer version, in J. M. Combes et al. (eds.), *Wavelets, Time-Frequency Methods and Phase Space*, Springer-Verlag, Berlin, pp. 313–27.

Mallat, S. (1989b), Theory for multiresolution signal decomposition: The wavelet representation, *Pattern Analysis and Machine Intelligence, Transactions of IEEE*, **11**(7), 674–93.

Omenzetter, P., Brownjohn, J. M. W. & Moyo, P. (2003), Identification of unusual events in multi-channel bridge monitoring data using wavelet transform and outlier analysis, *Proceedings of SPIE—The International Society for Optical Engineering*, **5057**, 157–68.

Robertson, A. N., Park, K. C. & Alvin, K. F. (1998a), Extraction of impulse response data via wavelet transform for structural system identification, *Journal of Vibration and Acoustics, Transactions of the ASME*, **120**(1), 252–60.

Robertson, A. N., Park, K. C. & Alvin, K. F. (1998b), Identification of structural dynamics models using wavelet-generated impulse response data, *Journal of Vibration and Acoustics, Transactions of the ASME*, **120**(1), 261–6.

Ruzzene, M., Fasana, A., Garibaldi, L. & Piombo, B. (1997), Natural frequencies and dampings identification using wavelet transform: Application to real data, *Mechanical System and Signal Processing*, **11**(2), 207–18.

Safak, E. & Celebi, M. (1991), Seismic response of Transamerica building, II: System identification, *Journal of Structural Engineering, ASCE*, **117**(8), 2405–25.

Satio, T. & Yokota, H. (1996), Evaluation of dynamic characteristics of high-rise buildings using system identification, *Journal of Wind Engineering and Industrial Aerodynamics*, **59**(2–3), 299–307.

Schoenwald, D. A. (1993), System identification using a wavelet-based approach, in *Proceedings of the 32nd IEEE Conference on Decision and Control*, San Antonio, TX, pp. 3064–5.

Strang, G. (1993), Wavelet transforms versus Fourier transforms, *Bulletin of the American Mathematical Society*, **28**(2), 288–305.

Todorovska, M. I. & Hao, T. Z. (2004), Presentation and compression of structural vibration monitoring data using wavelets as a tool in data mining, in *Proceedings of 13th World Conference on Earthquake Engineering*, Vancouver, Canada, Paper No. 2954.

Unser, M. & Aldroubi, A. (1996), Review of wavelet transforms for pattern recognitions, *Proceedings of SPIE, The International Society for Optical Engineering*, **2762**, 2–22.

VanDerVeen, A., Deprettere, E. F. & Swindlehurst, A. L. (1993), Subspace-based signal analysis using singular value decomposition, *Proceedings of the IEEE*, **81**(9), 1277–308.

Vold, H., Kundrat, J., Rocklin, G. T. & Russell, R. (1982), A multiple-input modal estimation algorithm for minicomputer, *SAE Transaction*, **91**(1), 815–21.

Wei, H. L. & Billings, S. A. (2002), Identification of time-varying systems using multiresolution wavelet models, *International Journal of System Science*, **33**(15), 1217–28.

Yang, Y. B., Tsai, I. C., Kao, C. C., Chen, C. H. & Huang, C. S. (2000), Dynamic and static monitoring and analysis of Shi-Tsang bridge, *Final Report to Bureau of Civilian Housing and City Planning*, Taipei, Taiwan (in Chinese).

Yeh, S. C., Cheng, C. P. & Loh, C. H. (1999), *Shaking Table Tests on Scales Down Five-Storey Steel Structures*, Rep. No. NCREE-99-002, National Center for Research on Earthquake Engineering, R. O. C. (in Chinese).

Zhou, Z. & Adeli, H. (2003), Time-frequency signal analysis of earthquake records using Mexican hat wavelets, *Computer-Aided Civil and Infrastructure Engineering*, **18**(5), 379–89.